Vol.67: e24220259, 2024
https://doi.org/10.1590/1678-4324-2024220259
ISSN 1678-4324 Online Edition

BABT
Brazilian Archives of Biology and Technology

Article - Engineering, Technology and Techniques

The Optical Degradation Characteristics of the Nanoparticles-Modified $BaSO_4$ Powder under Irradiation with Electrons and Protons

Mikhail Mikhailovich Mikhailov[1]
https://orcid.org/0000-0003-0657-1122

Semyon Alexandrovich Yuryev[1]*
https://orcid.org/0000-0003-4876-9284

Alexey Nikolaevich Lapin[1]
https://orcid.org/0000-0001-7203-9236

[1]Tomsk State University of Control Systems and Radioelectronics, Laboratory of Radiation and Space Materials Science, Tomsk, Russian Federation

Editor-in-Chief: Alexandre Rasi Aoki
Associate Editor: Andressa Novatski

Received: 07-Apr-2022; Accepted: 27-Feb-2024

*Correspondence: yusalek@gmail.com. (S.A.Y)

HIGHLIGHTS

- The composition, structure, and optical properties of nano-modified $BaSO_4$ powder under electron and proton irradiation were investigated.
- The diffuse reflectance spectra were recorded in vacuum after each irradiation period.
- Simultaneous irradiation changes the optical properties more expressively than separate one.
- The mechanism of absorption centers' formation under irradiation is suggested.

Abstract: The work presents the study of synergistic effects in changing of 1) the diffuse reflectance spectra within 0.2-2.2 µm and 2) the solar absorptance of barium sulfate ($nBaSO_4$) modified by silicon dioxide nanoparticles under separate and simultaneous irradiation with 30 keV electrons and 5 keV protons. The spectra were recorded before and after each irradiation period in vacuum at the site of irradiation (in situ). It was found that the change in optical properties of the powder under simultanous irradiation is larger in comparison with the total change under separate irradiation, with the values of electron fluence varying up to $F_e=9\cdot10^{16}$ cm^{-2} and the values of proton fluence varying up to $F_p=6\cdot10^{16}$ cm^{-2}. The difference reaches 1.24 times. The work provides the description of formation and accumulation of absorption centers under separate and sumultaneous irradiation of $nBaSO_4$.

Keywords: barium sulfate; silicon dioxide; nanoparticles; irradiation; optical properties.

INTRODUCTION

In many areas of industry, materials in the field are frequently affected by more than one external factor. These factors may act separately, sequentially, and simultaneously. The changes in the properties of

materials under the effect of external factors need to be thoroughly considered in terms of their application in space industry because when designing spacecraft an excessive reserve in operating characteristics will lead to a significant increase of construction weight, size, and cost. The inaccurate prediction of changes in the properties of materials might result in the early failure of spacecraft.

The external factors in space orbits are different kinds of irradiation (electrons, protons, and solar spectrum quanta), vacuum, and temperature. The change in the properties of materials under simultaneous action of several factors differs from the total change under their separate action. The studies on synergistic effects caused by the effect of external factors on spacecraft materials showed [1-4] that the former may manifest differently depending on the material. Studying synergistic effects in order to create the prediction basis for the materials' operating characteristics has recently gained significance thanks to the development of unmanned satellites, frame satellites, and nanosatellites, and because of the continuous increase in the active lifetime of regular satellites. Reduction of spacecraft weight and size is a topical issue related with optimizing the parameters of spacecraft based on the regularities of changing in operating characteristics under the simultaneous action of irradiation.

The recent studies [5,6] have shown the potential of barium sulfate powder as a pigment for thermal control coatings of spacecraft because of its reflectance capacity, which is higher than that of the pigments currently in use. In addition, $BaSO_4$ powders are widely used in various branches of industry [7-9]: paint and varnish, pulp and paper, construction, instrument engineering, oil, and many others. Furthermore, these powders are known as relatively common and cheap.

A very important characteristic of spacecraft materials is their radiation stability, which may be improved via modification with nanoparticles [10-14]. The experimental studies helped to find the types, optimal concentrations, and modes of introducing the modifying additives, which allow for a significant increase in radiation stability of barium sulfate micropowders, almost without a loss in reflectance capacity. The most efficient modifying additive is 3 wt.% SiO_2 nanopowder [15].

The purpose of this work is to study the synergistic effects under separate and simultaneous irradiation of SiO_2 nanoparticles-modified $BaSO_4$ ($nBaSO_4$) powder with electrons and protons using the change of 1) diffuse reflectance spectra (ρ_λ) within 200 to 2200 nm registered in vacuum at the irradiation site (in situ) and 2) solar absorptance (α_s).

MATERIAL AND METHODS

For the present study, the authors used $BaSO_4$ powder ("Extra pure reagent", average size 0.9 µm, purchased from Nacalai Tesque inc., Japan) modified with SiO_2 nanopowder (purity 99.8%, average size 10-12 nm, surface area 180-220 m2 / g, purchased from "Plasmoterm" LLC, Russia) in a ratio of 100:3. In order to modify, silicon dioxide nanopowder was dissolved in distilled water exposed to ultrasonic waves. Next, barium sulfate micropowder was added, and a mixture was stirred for 3 hours with magnetic stirrer. A mixture obtained was dried at 150°C in oven, ground in agate mortar, and heated for 2 hours in muffle furnace under 800°C (optimal modification temperature) [16]. After cooling down, the obtained powder of nBaSO4 was repeatedly ground in agate mortar.

The structure of modified $nBaSO_4$ was analyzed before and after irradiation in various modes with XRD-6100 X-ray diffractometer (Shimadzu, Japan). IR reflection spectra within 400 to 4000 cm^{-1} were recorded with Shimadzu IRTracer-100 IR-Fourier spectrometer equipped with DRS-8000A diffuse reflectance accessory. Before irradiation, a small portion of modified $nBaSO_4$ powder was sampled for analysis.

After separate or simultaneous irradiation, a portion sufficient for the registration of IR spectra was scraped off the surface layer of the powders pressed. Because three different radiation-exposed samples were employed, a few differences could be traced caused by uneven distribution of SiO_2 nanoparticles on the surface and by unequal concentration of OH groups and gases sorbed on the surface. These differences might have resulted in the different intensities of absorption bands in IR spectra.

The studies of $nBaSO_4$ powder spectra (ρ_λ) before and after irradiation were carried out in the "Spektr", the outer space conditions simulator [17]. Samples were prepared by pressing $nBaSO_4$ powder into substrates with 24 mm diameter and 4 mm height under a pressure of 1 MPa with 2 minutes exposure period. A pressure this low was chosen because of experimental data showing its effect on radiation stability of pigments [18]. Recording ρ_λ spectra from 200 to 2200 nm at irradiation site (in situ) was performed after each irradiation period in vacuum not lower than $P = 5 \cdot 10^{-6}$ torr at a temperature not exceeding 303K. Irradiation was carried out by 30 keV electrons and by 5 keV protons. Solar absorptance (α_s) was calculated via ρ_λ in accordance with international standards [19, 20].

Mathematical modeling of the pathways for charged particles was performed using CASINO (monte CArlo SImulation of electroN trajectory in sOlids) [21] and SRIM (the Stopping and Range of Ions in Matter)

software [22]. When modeling using programs, $BaSO_4$ compound with a density of 4.5 g/cm^3 was selected as a target. In CASINO, electron energy was specified to be 30 keV whereas beam diameter was 100 nm; in SRIM protons energy was specified to be 5 keV.

RESULTS AND DISCUSSION

The study of $nBaSO_4$ powders structure

Studies of $nBaSO_4$ powders structure were carried out before irradiation and after separate and simultaneous irradiation with electrons and protons. Figure 1 shows an example of XRD spectra for modified barium sulfate powder before and after simultaneous irradiation with electrons and protons with a fluence of $6.73 \cdot 10^{16}$ and $3.36 \cdot 10^{16}$ cm^{-2}, respectively. All of the XRD data obtained show peaks corresponding to the phase of orthorhombic crystalline barium sulfate. SiO_2 nanopowder occurring in the samples under analysis does not have reflection peaks in XRD spectra because of its amorphous structure. In the analysis of XRD spectra of $nBaSO_4$ powder obtained before irradiation and after separate and simultaneous action of electrons and protons, it was found that irradiation does not cause the occurrence of additional phases and significant changes in structure.

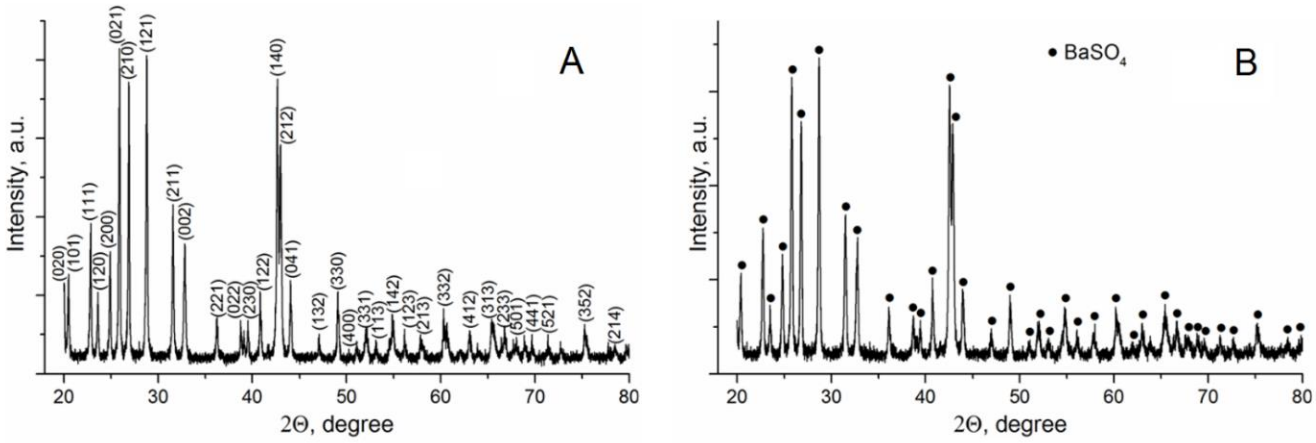

Figure 1. X-ray diffraction patterns of $nBaSO_4$ powder before irradiation (A) and after simultaneous irradiation with electrons and protons (B).

The study of IR reflection spectra

The authors studied the reflectance spectra in the IR region of $nBaSO_4$ powder before and after separate and simultaneous irradiation with electrons and protons. Kubelka-Munk transformation [23] was implemented and valuated to maximum intensity peak at 1132 cm^{-1}. Figure 2 shows an example of IR spectra for modified barium sulfate powder before and after irradiation with e^- and p^+ with a fluence of $6.73 \cdot 10^{16}$ and $3.36 \cdot 10^{16}$ cm^{-2}.

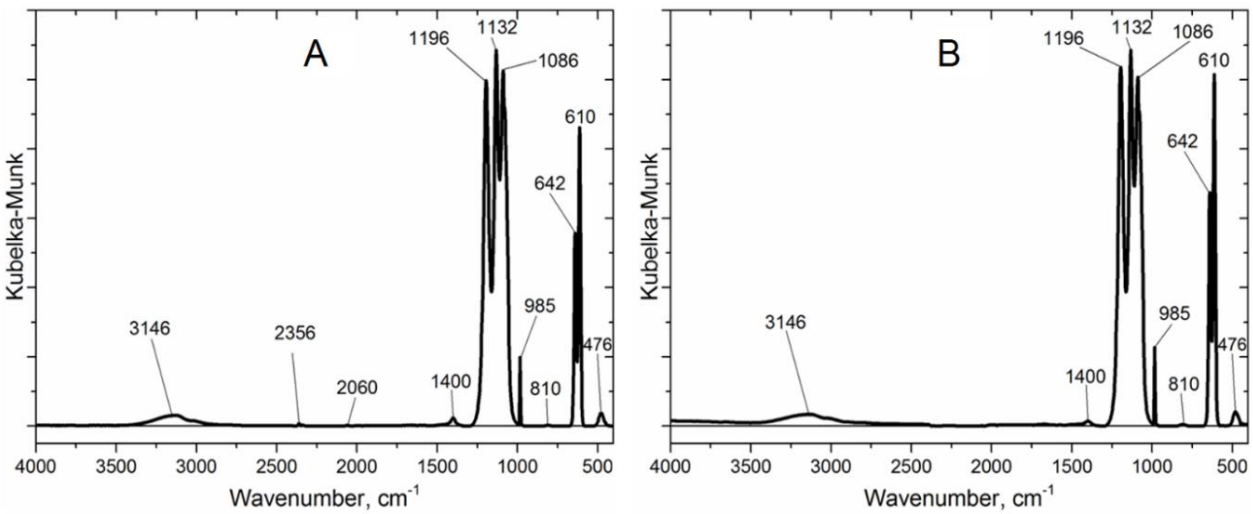

Figure 2. IR spectra of $nBaSO_4$ powder before (A) and after simultaneous irradiation with electrons and protons (B).

The highest intensity pertains to the bands (Table 1) pre-determined by a different types of fluctuation in SO_4^{2-} centers [24-28]: the bands at 610 and 642 cm^{-1} are determined by out-of-plane bending; the band at 985 cm^{-1} is determined by symmetric stretching; the three bands within the region from 1080 to 1200 $см^{-1}$ are caused by symmetric and asymmetric stretching and bending. The band at 2060 cm^{-1} is related to fluctuations of sulfur-containing oxygen. The weak band at 2325-2360 cm^{-1} with two peaks corresponds to fluctuations of atmospheric carbon dioxide. The wide absorption band at 3146 cm^{-1} is determined by OH groups on the sample surface.

Table 1. Intensities of peaks (relative units) in the IR spectra of $nBaSO_4$ powder under separate and simultaneous irradiation with electrons and protons.

Irradiation mode	**Wavenumber, cm^{-1}**											
	476	610	642	810	985	1086	1132	1196	1400	2060	2356	3146
Before	0.036	0.862	0.544	0.003	0.107	1.026	1.086	0.998	0.024	0.002	0.007	0.031
e^-	0.049	0.823	0.504	0.016	0.138	1.041	1.086	0.996	0.006	0.014	0.005	0.001
p^+	0.061	0.819	0.580	0.019	0.273	1.025	1.086	1.039	0.005	0.017	0.004	0.002
$e^- + p^+$	0.041	1.015	0.674	0.005	0.228	1.007	1.086	1.036	0.015	0.001	0.001	0.034

The bands typical of SiO_2 compounds are located approximately in the same region of wavenumbers [29-32]:

- fluctuations of bridging Si-O-Si oxygen at 460, 810, and 1110 cm^{-1} and symmetric Si-Si valence fluctuations at 615 cm^{-1};
- torsional fluctuations of SiO_2 at 805 cm^{-1}.

As seen from the data in Table 1, the authors can argue that

1) During separate irradiation with protons and electrons, the band intensity at 476, 810, and 2060 cm^{-1} increases while the intensity of bands at 610, 3146, and 1400 cm^{-1} decreases;
2) During simultaneous irradiation, the intensity of bands at 476, 810, 2060, and 3146 cm^{-1} does not significantly change while the intensity of bands at 610, 642, 985, and 1196 cm^{-1} increases, and the intensity of bands at 1086 and 1400 cm^{-1} decreases;
3) The large increase of band intensity at 642, 985, and 1196 cm^{-1} occurs during separate irradiation with protons and simultaneous irradiation with protons and electrons whereas for the band at 1086 cm^{-1} intensity decreases in the abovementioned irradiation modes;
4) Irradiation with electrons leads to a decrease in the band intensity with the peaks at 642 and 1196 cm^{-1} and to its increase at 985 and 1086 cm^{-1}.

Study of diffuse reflectance spectra within the 0.2-2.2 μm

Irradiation with electrons

The authors examined ρ spectra and Δρ difference spectra, which are determined by the difference between ρ spectra before and after irradiation, and are represented by the spectra of irradiation-induced absorption (Figure 3). The reflectance of non-irradiated powder from 400 to 1400 nm approximates 95%. Solar absorptance (α_s) calculated by ρ spectra of $nBaSO_4$ powder equals 0.048 before irradiation.

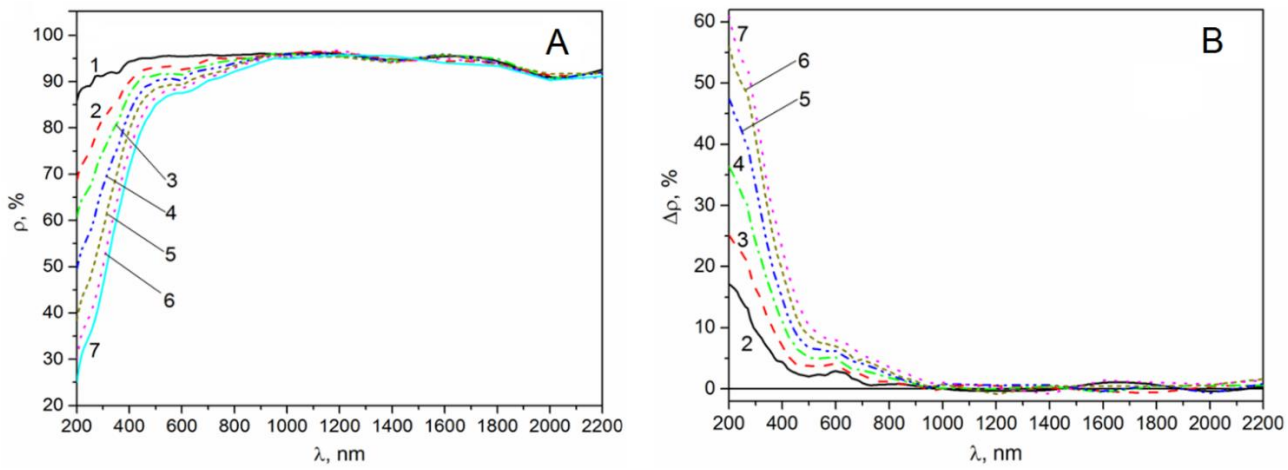

Figure 3. ρ (A) and Δρ (B) spectra before (1) and after irradiation of the $nBaSO_4$ powder with electron fluence,·10^{16} cm^{-2}: 0.5(2); 1.5(3); 3(4); 5(5); 7(6), 9(7).

When irradiating by electrons, the reflectance significantly decreases within the region from 200 to 1000 nm, and the most significant changes occur from 200 to 500 nm. From 800 to 2200 nm, changes are insignificant and do not exceed 5%. The Δρ spectra (Figure 3B) show that maximum change occurs at a wavelength of 200 nm where the reflectance reaches 61% at maximum fluence. In the visible spectrum region, the absorption band appears with the maximum at 600 nm and disappears as fluence increases. The shape and non-elementary character of absorption bands from 200 to 900 nm allow assuming that several types of intrinsic defects occur in $nBaSO_4$ powders, which absorb in the UV and in the visible spectrum regions.

The correlation between the changes in solar absorptance ($\Delta\alpha_s$) and electron fluence (Table 2) shows its gradual increase. Its maximum value equals 0.072 with a fluence of $F=9\cdot10^{16}cm^{-2}$.

Table 2. The correlation between changes in the solar absorptance (α_s) of the $nBaSO_4$ powder and the electron fluence under separate irradiation

F_e-, cm^{-2}	$0.5\cdot10^{16}$	$1.5\cdot10^{16}$	$3\cdot10^{16}$	$5\cdot10^{16}$	$7\cdot10^{16}$	$9\cdot10^{16}$
$\Delta\alpha_s$	0.018	0.027	0.038	0.049	0.059	0.072

Irradiation with protons

When irradiating by 5 keV protons, the reflectance changes primarily in the visible spectrum region (Figure 4). When increasing proton fluence, the reflectance significantly decreases. Similar to the irradiation with electrons, the major changes occur in the UV spectrum region. With maximum protons fluence ($F=6\cdot10^{16}cm^{-2}$), the Δρ value reaches 60%. It decreases during the transition to the visible spectrum region. The difference between Δρ spectra and spectra for electron irradiation lies in the fact that the long-wave front of the absorption band is narrower. In the area of 600 nm, the changes in reflectance are almost nonexistent. This might be the evidence of a fewer number of absorption centers' types during irradiation with protons.

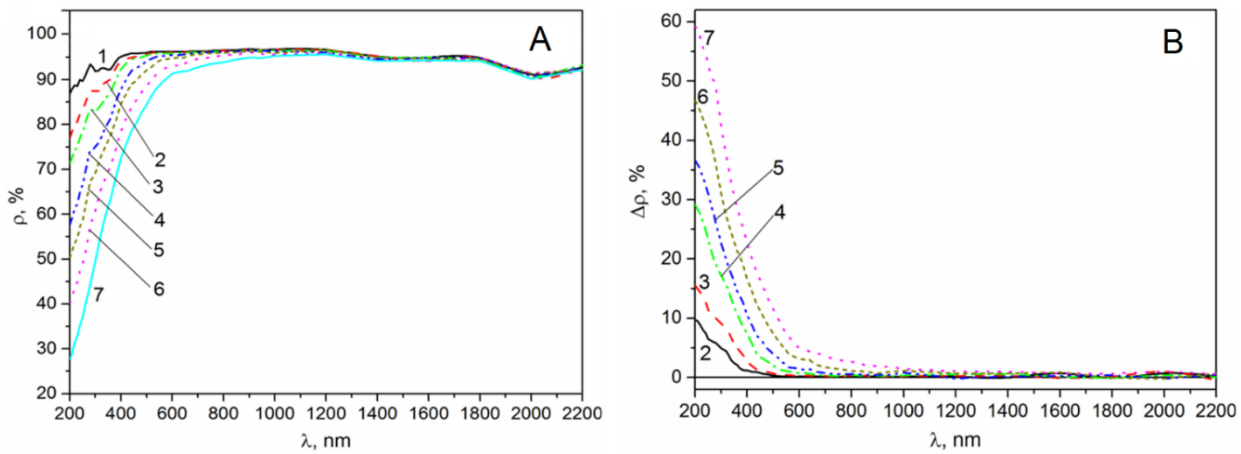

Figure 4. ρ (A) and Δρ (B) spectra before (1) and after irradiation of the $nBaSO_4$ powder with proton fluence, ·10^{16} cm^{-2}: 0.3 (2); 1 (3); 2 (4); 3 (5); 4.5 (6), 6 (7).

The values of changes in $\Delta\alpha_s$ when irradiating by protons (Table 3), calculated from $\Delta\rho$ spectra, show the increase in the coefficient with the increase in proton fluence. At small and equal values of the fluence, significant changes occur for irradiation with electrons. With the increase in the fluence to $5\cdot10^{16}$ cm^{-2}, the irradiation with protons results in significant changes and reaches 0.066, which is higher than the value for irradiation with electrons (Table 2).

Table 3. The correlation between changes in the solar absorptance (α_s) of the $nBaSO_4$ powder and the proton fluence under separate irradiation

F_p+, cm^{-2}	$0.3\cdot10^{16}$	$1\cdot10^{16}$	$2\cdot10^{16}$	$3\cdot10^{16}$	$4.5\cdot10^{16}$	$6\cdot10^{16}$
$\Delta\alpha_s$	0.003	0.006	0.014	0.025	0.042	0.066

As well as for irradiation with electrons, the $\Delta\alpha_s$ values for irradiation of $nBaSO_4$ powder by protons are relatively low in comparison with other pigments that are applied for previously studied "solar reflector" thermal control coatings [33, 34]. It allows concluding on the effective stability of barium sulfate powder modified by SiO_2 nanoparticles when exposed to the action of electrons and protons.

Simultaneous irradiation with electrons and protons

Measurements of the diffuse reflectance spectra of $nBaSO_4$ powder were carried out with simultaneous irradiation with electrons and protons (Figure 5). Within 200-1400 nm spectrum range, a decrease in the reflectance coefficient is observed, and in the longer wavelength region its slight increase (about 2%) can be traced. As in the case of separate irradiation with electrons and protons, the largest decrease in the reflectance coefficients is recorded in the UV region of the spectrum with a peak at 200 nm. The maximum value of $\Delta\rho$ reaches 66% at a wavelength of 200 nm. The long-wavelength front of the absorption band qualitatively coincides with the one for the irradiation with electrons: it is protracted into the IR region, and a protrusion at about 600 nm is clearly observable. In the region above 1400 nm, the reflectance coefficient does not change.

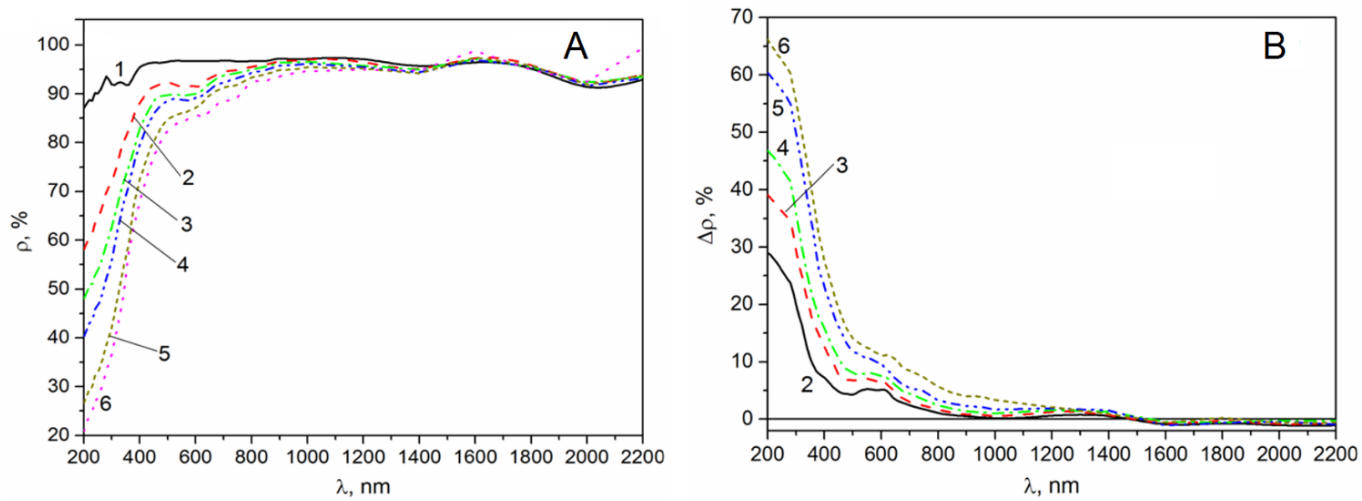

Figure 5. ρ (A) and Δρ (B) spectra before (1) and after simultaneous irradiation of the $nBaSO_4$ powder with the fluence of electrons and protons, $\cdot10^{16}$ cm^{-2}: 1 + 0.37 (2); 2.1 + 0.93 (3); 3 + 1.35 (4); 5 + 2.42 (5); 6.73 + 3.36 (6).

The $\Delta\alpha_s$ values of $nBaSO_4$ powder depending on the time of simultaneous irradiation with electrons and protons are given in Table 4. In addition, Table 4 contains comparative values of $\Delta\alpha_s$ for separate irradiation, as well as the values of the additivity coefficient (C_{add}) calculated as the ratio of $\Delta\alpha_s$ values for simultaneous irradiation ($\Delta\alpha_{ssim}$) to the sum of $\Delta\alpha_s$ values for separate irradiation with electrons and protons ($\sum\Delta\alpha_s$):

$$C_{add} = \Delta\alpha_{ssim} / \sum\Delta\alpha_s. \quad (1)$$

Table 4. The correlation between changes in the solar absorptance, additivity coefficient, and the time of simultaneous irradiation of the $nBaSO_4$ powder with electrons and protons

Simultaneous irradiation time, hours		1	2.1	3	5	6.73
F_{e^-}, cm^{-2}		$1\cdot10^{16}$	$2.1\cdot10^{16}$	$3\cdot10^{16}$	$5\cdot10^{16}$	$6.73\cdot10^{16}$
F_{p^+}, cm^{-2}		$0.37\cdot10^{16}$	$0.93\cdot10^{16}$	$1.35\cdot10^{16}$	$2.42\cdot10^{16}$	$3.36\cdot10^{16}$
$\Delta\alpha_s$	**e^-**	0.019	0.028	0.035	0.047	0.057
	p^+	0.004	0.006	0.009	0.019	0.029
	$e^- + p^+$	0.028	0.042	0.054	0.078	0.094
	$\sum\Delta\alpha_s$	0.023	0.034	0.044	0.066	0.086
$C_{add}=\Delta\alpha_{ssim}/\sum\Delta\alpha_s$		1.22	1.24	1.23	1.18	1.09

The data in the tables show that

1) At the given values of energy and fluence, electrons make a significantly greater contribution to the degradation of the $nBaSO_4$ powder optical properties in comparison with that of protons;

2) Of the three modes of irradiation, the largest changes in $\Delta\alpha_s$ occur for the simultaneous irradiation with electrons and protons, and the most insignificant changes are caused by the irradiation with protons;

3) With the same irradiation period, simultaneous irradiation leads to more significant changes in the absorption coefficient in comparison with the sum of changes induced by separate irradiation with electrons and protons;

4) The additivity coefficient is greater than unity at any irradiation time, and its largest value (C_{add} = 1.24) correlates with 2 hour long irradiation period, an electron fluence F = $2.1\cdot10^{16}$ cm^{-2}, and a proton fluence F = $0.93\cdot10^{16}$ cm^{-2}.

Comparing the contribution of electrons and protons to $\Delta\alpha_s$ values (Figure 6), the authors can argue that at a short irradiation time, the contribution of protons to the degradation of the $nBaSO_4$ powder optical properties is up to 4.75 times lower than that of electrons. With an increase in the irradiation time, this difference decreases, and at a maximum irradiation time of 6.73 h reaches 1.97 times. The largest changes in $\Delta\alpha_s$ (0.094) correlate with the longest period of simultaneous irradiation with electrons and protons (6.73 h). In this case, the sum of $\Delta\alpha_s$ values for separate irradiation with electrons and protons reaches 0.086 (the same time, similar intensities).

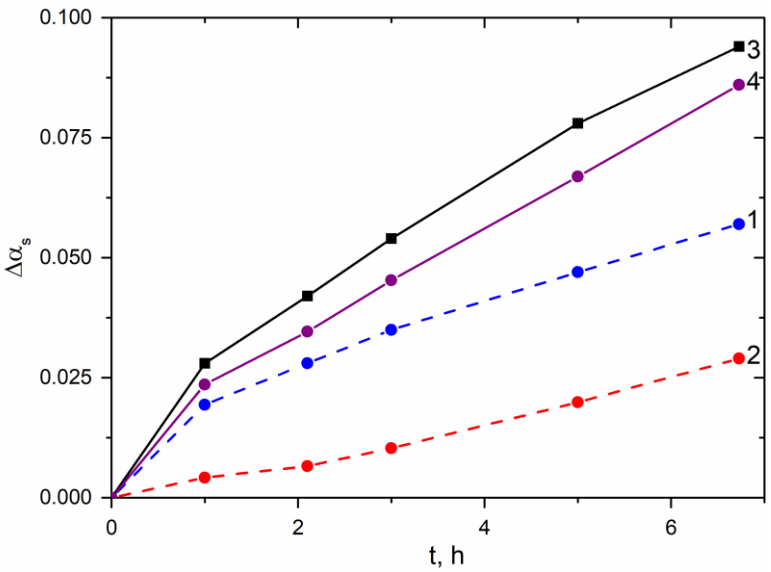

Figure 6. Correlation between changes in the solar absorptance (α_s) of the $nBaSO_4$ powder obtained by calculations based on the experimental values: under separate irradiation with electrons (1), protons (2), under simultaneous irradiation with electrons and protons (3), the sum of Δa_s values under the separate action of electrons and protons (4).

Thus, an estimation of degradation based on the results of separate irradiation would lead to 1.23 times underestimation for 3 h and 1.09 times for the maximum irradiation time. The underestimation of changes in the main operating characteristic ($\Delta\alpha_s$) can lead to an increase in the temperature of spacecraft if $nBaSO_4$ powder is to be applied as a pigment for thermal control coatings of spacecraft.

Analysis of the irradiation-induced processes resulting in the degradation of the $nBaSO_4$ powder optical properties

Judging by induced absorption spectra during separate and simultaneous irradiation of the $nBaSO_4$ powder with electrons and protons (Figures 3, 4, and 5), the main changes occur in the UV and visible regions with $\Delta\rho$ maximum at 200 nm. In this region, intrinsic defects of the anionic sublattice (such as SO_4^-, SO_3^-, SO_2^-, and O^-) initiate the absorption [35 - 39]. At low fluence of electrons or protons, the absorption band is narrow; with an increase in fluence, it broadens to longer wavelengths. In this case, a protrusion is recorded (about 600 nm).

The electron energy E = 30 keV is insufficient to displace the atoms of $nBaSO_4$ cationic and anionic sublattices from the crystal lattice sites. Therefore, the main and only mechanism of their interaction is ionization process. The path for electrons with such energy does not exceed 5 µm (Figure 7).

The main losses of protons with energy E = 5 keV are determined by elastic collisions with lattice atoms followed by the formation of anionic and cationic vacancies and interstitial anions and cations in different charge states. There are almost no ionization losses. The path for protons of this energy is less than 200 nm (Figure 7).

The primary defects are electron / hole pairs being the result of ionization processes upon irradiating $nBaSO_4$ compounds – as well as oxide compounds – with electrons and protons.

$$MeO + (e^-, p^+) \rightarrow Me^{2+} + O^{2-} \quad (2)$$

$$BaSO_4 + (e^-, p^+) \rightarrow Ba^{2+} + SO_4^{2-} \quad (3)$$

SO_4^{2-} centers decompose forming other hole centers.

$$SO_4^{2-} \rightarrow SO_4^- + e^- \quad (4)$$

$$SO_4^{2-} \rightarrow SO_3^{2-} + O \quad (5)$$

$$SO_3^{2-} + e^- \rightarrow SO_3^- \quad (6)$$

$$SO_3^{2-} \rightarrow SO_2^- + O^- \quad (7)$$

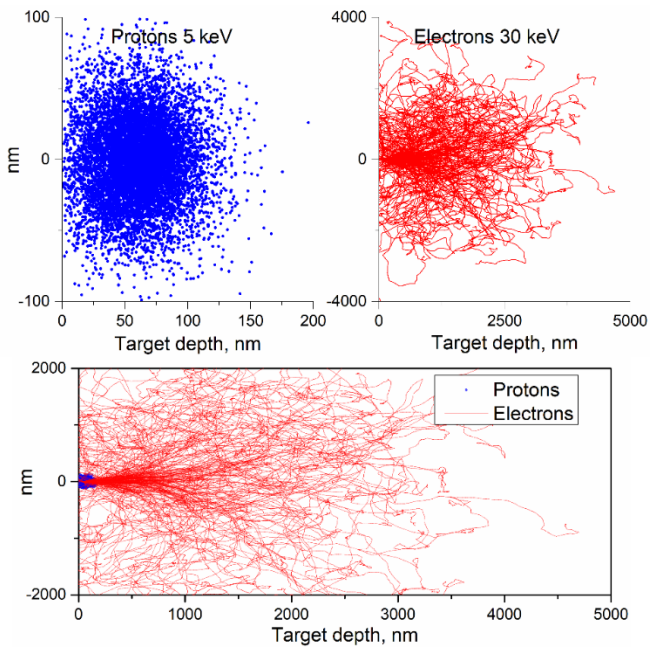

Figure 7. Path of 5 keV protons and 30 keV electrons in $BaSO_4$.

In addition to those formed by irradiation, $BaSO_4$ powders contain non-stoichiometric SO_4^{2-} absorption centers. When they decompose, energy electrons are released, and they can decompose other SO_4^{2-} centers forming the same absorption centers as in reactions (4-7): SO_4^-, SO_3^-, SO_2^-, O^- , and O. These centers absorb quanta in UV and visible regions of the spectrum.

If SO_4^{2-} centers are the primary defects of the anionic sublattice formed under the action of radiation or during autodecomposition of non-stoichiometric SO_4^{2-}, SO_4^-, SO_3^-, SO_2^-, O^-, and O are secondary absorption centers. The positions of the absorption bands for some of these centers are currently established: 380nm (SO_3^-), 575nm (SO_2^-), and 620 nm (O^-) [35 - 39]. Their values show that as the structure of these centers is simplified, the wavelength of the absorption bands' peaks (caused by these centers and their ionization energy) increases.

This correlation can be linked – to a certain extent – to the correlations known in radiation physics. For example, in alkali halide crystals, the band of irradiation-induced primary defects and color centers of the anionic sublattice (F-centers) is located in the shorter wavelength part of the spectrum compared to its combinations (R, M, and other more complex centers) [40]. In TiO_2, F-centers absorb within 800–1200 nm, and F^+ centers absorb in the 1740 nm region [41]. In ZnO, F-centers absorb in the 410 nm region, and F^+ centers absorb in the 560 nm region [42]. Therefore, it can be assumed that the absorption band of SO_4^- centers is located in a shorter wavelength region in comparison with the bands of SO_3^-, SO_2^-, and absorption centers.

The bands of absorption centers determined by defects of the cationic sublattice in TiO_2 ZnO, and ZrO_2 [41 - 43] are located in a shorter wavelength region in comparison with the bands for defects in the anionic sublattice. By analogy with the absorption bands of the abovementioned oxides, it can be assumed that the absorption bands for the absorption centers 1) of ions in different charge states and 2) of barium atoms in $BaSO_4$ are located in a shorter wavelength region compared to the bands of defects in the anionic sublattice. This region of the spectrum varies from λ<200 nm to $\lambda > \lambda_g$. Therefore, we can conclude that changes in the solar absorptance (α_s) of $BaSO_4$ powder are determined only by changes in the concentration of anionic defects such as SO_4^- , SO_3^-, SO_2^-, and O^-.

The regularities of the change in the concentration of absorption centers with the $\Delta\alpha_s$ values were compared with the change in the intensity of the IR absorption bands under separate and simultaneous irradiation with electrons and protons of the $nBaSO_4$ powder. The change in the intensity of these bands changes qualitatively and quantitatively according to various trends: it decreases, increases, and remains unchanged; the changes are small or large. Therefore, it is difficult to detect which processes will determine the increase in the concentration of these absorption centers during irradiation. After the final irradiation period (6.73 h), the additivity coefficient is 1.09 according to the $\Delta\alpha_s$ values (Table 4), i.e., simultaneous irradiation provides large changes (0.094) compared to the total change for separate irradiation (0.086). The change in the intensity of three powerful absorption bands at 1086, 1132, and 1196 cm^{-1} provides the additivity coefficient of less than unity, which is opposite to the change in the concentration of absorption centers and of α_s. Therefore, they cannot be a measure of the optical degradation degree for $nBaSO_4$ powder under irradiation with protons and electrons of such energies. This correlation is consistent with the change in the intensity of absorption bands at 610 cm^{-1} and 642 cm^{-1} determined by interplanar bending.

The changes in the intensity of the absorption bands at 476, 810, and 1110 cm^{-1} determined by the vibrations of the bridging Si-O-Si oxygen, as well as the band at 610 cm^{-1} determined by the symmetric stretching of Si-Si, are qualitatively opposite to the changes in the absorption coefficient α_s. Therefore, they can only confirm the fact that silicon dioxide is present in this compound, and its fluctuations change in intensity with all the irradiation types.

The concentration of OH groups decreases under separate irradiation with protons and electrons and increases under their simultaneous action. A decrease is determined by their desorption under the action of radiation while an increase is determined by their formation during the interaction of radiation with a powder.

They can form via two channels. First, water molecules on the surface and in the bulk decompose under the action of radiation and form OH groups and atomic hydrogen. Such radicals have a significant effect on the recombination processes in the sulfate subsystem when exposed to radiation. On the one hand, they suppress them, on the other hand, they lead to the appearance of a new channel for the decomposition of complex anions. Quantum chemistry methods show that atomic hydrogen forms stable complexes with SO_4^- and SO_3^-. When the SO_4^{2-} anion interacts with atomic hydrogen, SO_3^- and OH^- ions are formed without activation [34-38].

The second channel is determined by the fact that hydrogen atoms, which appear as a result of thermalization of protons at the depth of their path, can participate in the formation of OH groups under simultaneous irradiation. The oxygen atoms and ions required are formed during ionization processes under

the action of electrons (expressions 3-8). Therefore, along with desorption of OH groups bound to the surface of the $nBaSO_4$ powder by gravity and electron bonding, their formation occurs in approximately the same amount under simultaneous irradiation.

As a result, the following regularities of the change in optical properties were observed under the simultaneous action of protons and electrons:

1) the intensity of the absorption band at 3146 cm^{-1} remains approximately the same as before irradiation;

2) additional amount of SO_4^{2-}, SO_4^-, SO_3^-, SO_2^-, and O^- ions is formed (in comparison with the amount formed under the separate action of protons / electrons in the same irradiation modes);

3) the intensity values of the absorption bands and the solar absorptance (α_s) exceed the total value under separate irradiation;

4) the additivity coefficient is greater than unity for all values of electron and proton fluences.

5) Weak-intensity bands of sulfur-containing oxygen (2060 cm^{-1}) and carbon dioxide (2356 cm^{-1}) show a small amount of corresponding fluctuations.

Thus, from the entire set of absorption bands in the IR region (from 500 to 4000 cm^{-1}), one can evaluate the patterns of change in the concentration of absorption centers and the additivity coefficient under separate and simultaneous irradiation of the $nBaSO_4$ powder only by the change in the intensity of absorption bands at 610 cm^{-1} and 642 cm^{-1}, which are determined by interplanar bending of SO_4^{2-} centers. The rest of the bands can serve as indicators for the presence of respective absorption centers in the present study.

CONCLUSION

The changes in the composition, structure, and diffuse reflectance spectra in the UV, visible, near IR, and IR spectrum regions have been studied under separate and simultaneous irradiation with 30 keV electrons and 5 keV protons of a micron-sized $BaSO_4$ powder modified with SiO_2 nanoparticles. The study was carried out via recording diffuse reflectance spectra within 0.2 - 2.2 µm in vacuum at the irradiation site (in situ). The energies were selected considering the fact that in high orbits of spacecraft (geostationary orbit, r = 36000 km, high elliptical orbit, r_1 = 400 km, r_2 = 40000 km) – as well as in other regions of the solar system – such particles have maximum fluxes and show the most significant change in optical properties of the materials applied for the outer surfaces of the spacecraft.

In addition, the authors described the processes of formation and accumulation of absorption centers under separate and simultaneous irradiation of $nBaSO_4$. It is shown that bands are formed in the spectra of induced absorption within 200 nm to 600-800 nm caused by defects in the anionic sublattice of SO_4^{2-}, SO_4^-, SO_3^-, SO_2^-, and O^- because of ionization processes while irradiating with electrons and – mainly – elastic collisions while irradiating with protons. There is no absorption in the longer wavelength region. A certain contribution to the change in the optical properties can be made by OH groups formed both during the thermalization of protons and by water molecules existing before irradiation.

It was found that for all values of the electron fluence (up to $F_e = 9 \cdot 10^{16}$ cm^{-2}) and the proton fluence (up to $F_p = 6 \cdot 10^{16}$ cm^{-2}), the change in the solar absorptance ($\Delta\alpha_s$) of the $nBaSO_4$ powder is greater under simultaneous irradiation than the sum of changes under separate irradiation. The difference reaches 1.24 times.

Funding: This work was financially supported by the Ministry of Science and Higher Education of the Russian Federation (Goszadanie), No. FEWM-2023-0012.
Acknowledgments: The authors express their gratitude to E.V. Komarov, engineer of the Laboratory of Radiation and Space Materials Science, for invaluable assistance in performing experimental studies.
Conflicts of Interest: The authors declare no conflict of interest.

REFERENCES

1. Shuvalov VA, Tokmak NA, Pismennyi NI, Kochubey GS. [Synergetic effect of atomic oxygen flow and vacuum ultraviolet flux on spacecraft polyimide films]. Kosm nauka tehnol. 2012;18:10–9. Russian.
2. Mikhailov MM, Neshchimenko VV. Synergistic Effects in “Solar Reflectors” Thermal Control Coating Under GSO Simulated Conditions Exposure. In: Kleiman J, editor. Protection of Materials and Structures from the Space Environment, vol. 47, Cham: Springer International Publishing; 2017, p.149–58.
3. Miller SKR, Banks B. Degradation of Spacecraft Materials in the Space Environment. MRS Bull. 2010;35:20–4.
4. Shimamura H, Miyazaki E. Investigations into Synergistic Effects of Atomic Oxygen and Vacuum Ultraviolet. J Spacecr Rockets. 2009;46:241–7.
5. Mikhailov MM, Yuryev SA, Lapin AN, Lovitskiy AA. The effects of heating on $BaSO_4$ powders’ diffuse reflectance spectra and radiation stability. Dyes Pigments. 2019;163:420–4.
6. Mikhailov MM, Yuryev SA, Lapin AN. Prospects for applying $BaSO_4$ powders as pigments for spacecraft thermal control coatings. Acta Astronaut. 2019;165:191–4.
7. Cao R, Qin Z, Yu X, Wu D, Zheng G, Li W. Synthesis and luminescence properties of $BaSO_4$ phosphor activated with Sm. Optik. 2016;127:1126–9.
8. Annalakshmi O, Jose MT, Madhusoodanan U. Synthesis and characterisation of $BaSO_4$:Eu thermoluminescence phosphor. Radiat Prot Dosim. 2012;150:127–33.
9. Bahl S, Lochab SP, Pandey A, Kumar V, Aleynikov VE, Molokanov AG, et al. Characterization and luminescence studies of Eu doped Barite nanophosphor. J Lumin. 2014;149:176–84.
10. Delfini A, Pastore R, Santoni F, Piergentili F, Albano M, Alifanov O, et al. Thermal analysis of advanced plate structures based on ceramic coating on carbon/carbon substrates for aerospace Re-Entry Re-Useable systems. Acta Astronaut. 2021;183:153–61.
11. Bo Z, Gang L, Kangli C, Weimin C. Preparation and Space Environmental Stability of a Nano-Materials Modified Thermal Control Coating. In: Kleiman J, editor. Protection of Materials and Structures from the Space Environment, vol. 47, Cham: Springer International Publishing; 2017, p. 433–41.
12. Mikhailov MM. Optical features and the powders ZnO, TiO_2, $BaTiO_3$, $Gd_3Ga_5O_{12}$, modified by nanoparticles. Scientific Work. Volume 5. Publishing house of Tomsk State University of Control Systems and Radio Electronics; 2016. 308 p.
13. Li C, Liang Z, Xiao H, Wu Y, Liu Y. Synthesis of $ZnO/Zn_2SiO_4/SiO_2$ composite pigments with enhanced reflectance and radiation-stability under low-energy proton irradiation. Mater Lett. 2010;64:1972–4.
14. Mikhailov MM. Optical properties and radiation stability of Metal Oxide Powders modified with Nanoparticles. Volume 6. Publishing house of Tomsk State University of Control Systems and Radio Electronics; 2019. 312 p.
15. Mikhailov MM, Neshchimenko VV, Yuryev SA, Grigorevsky AV, Lovitskiy AA, Vashchenkov IS. On the Radiation Stability of $BaSO_4$ Pigment Modified with SiO_2 Nanoparticles and Applied for Spacecraft Thermal Control Coatings. DDF. 2018;386:277–82.
16. Mikhailov MM, Yuryev SA, Lovitskiy AA. On the correlation between diffuse reflectance spectra and particle size of $BaSO_4$ powder under heating and modifying with SiO_2 nanoparticles. Opt Mater. 2018;85:226-9.
17. Kositsyn LG, Mikhailov MM, Kuznetsov NY, Dvoretskii MI. Apparatus for study of diffuse-reflection and luminescence spectra of solids in vacuum, Instrum Exp Tech New York. 1985;28:929–32.
18. Mikhailov MM, Kuznetsov NYa. [Formation of color centers in ZrO_2 powders during pressing and subsequent irradiation]. Inorg Mater. 1988;24:785-89. Russian.
19. ASTM E490 - 00a Standard Solar Constant and Zero Air Mass Solar Spectral Irradiance Tables.
20. ASTM E903 – 20 Standard Test Method for Solar Absorptance, Reflectance, and Transmittance of Materials Using Integrating Spheres.
21. Demers H, Poirier-Demers N, Couture AR, Joly D, Guilmain M, de Jonge N, et al. Three-dimensional electron microscopy simulation with the CASINO Monte Carlo software. Scanning. 2011;33:135–46.
22. Ziegler JF, Ziegler MD, Biersack JP. SRIM – The stopping and range of ions in matter. Nucl Instrum Methods Phys Res B: Beam Interact Mater At. 2010;268:1818–23.
23. Kubelka P. Errata: New Contributions to the Optics of Intensely Light-Scattering Materials. J Opt Soc Am. 1948;38:448–57.
24. Vicum L, Mazzotti M, Baldyga J. Applying a Thermodynamic Model to the Non-Stoichiometric Precipitation of Barium Sulfate. Chem Eng Technol. 2003;26:325–33.
25. Sifontes ÁB, Cañizales E, Toro-Mendoza J, Ávila E, Hernández P, Delgado BA, et al. Obtaining Highly Crystalline Barium Sulphate Nanoparticles via Chemical Precipitation and Quenching in Absence of Polymer Stabilizers. J Nanomater. 2015;2015:1–8.
26. Zhang M, Zhang B, Li X, Yin Z, Guo X. Synthesis and surface properties of submicron barium sulfate particles. Applied Surface Science 2011;258:24–9.
27. Prameena B, Anbalagan G, Sangeetha V, Gunasekaran S, Ramkumaar GR. Behaviour of Indian natural barite mineral. Int J ChemTech Res. 2013;5:220–31.
28. Manam J, Das S. Thermally stimulated luminescence studies of undoped, Cu- and Mn-doped $CaSO_4$ compounds. Radiat Eff Defects Solids. 2008;163:955–65.

29. Borilo LP. [Synthesis and physicochemical regularities of the formation by the sol-gel method of thin-film and dispersed nanomaterials of oxide systems of elements of III - V groups] [dissertation]. Tomsk: Tomsk State University; 2003. 286 p. Russian.
30. Lange P. Evidence for disorder-induced vibrational mode coupling in thin amorphous SiO_2 films. J Appl Phys. 1989;66:201–4.
31. Ji Y, Jiang Y, Liu H, Wang L, Liu D, Jiang C, et al. Effects of thermal treatment on infrared optical properties of SiO_2 films on Si Substrates. Thin Solid Films. 2013;545:111–5.
32. Savchenko MO, Mysov OP, Chernenko IM, Oleynikov VG. Infrared absorption spectra of nanosized silica with organic additives. Odes'kyi Politechnichnyi Universytet Pratsi. 2014:185–90. 32.
33. Neshchimenko V, Li C, Mikhailov M, Lv J. Optical radiation stability of ZnO hollow particles. Nanoscale. 2018;10:22335–47.
34. Neshchimenko VV. [Investigation of the structure, properties and radiation resistance of oxide powders modified with nanoparticles] [dissertation]. Tomsk: Institute of Strength Physics and Materials Science SB RAS;2017.272 p. Russian.
35. Platonov AN. [The nature of the color of minerals]. Kiev: Naukova Dumka; 1976. 264 p. Russian.
36. Sharaf MA, Hassan GM. Radiation induced radical in barium sulphate for ESR dosimetry: a preliminary study. Nucl Instrum Methods Phys Res B: Beam Interact Mater At. 2004;225:521–7.
37. Bartoshinsky VZ, Shumsky AA, Larikov AL, Dersky LS. [Paramagnetic and optically active centers in barites of the Ukraine]. Mineralogicheskii Zhurnal. 1991;13:73-8. Russian.
38. Bernstein LR. Coloring mechanisms in celestite. Am Mineral. 1979;64:160–8.
39. Marfunin AS. Spectroscopy, Luminescence and Radiation Centers in Minerals. Springer; 1979. 356 p.
40. Mikhailov MM, Ardyshev VM, Belyakov MV. Oscillator strength of electron-type color centers in KCl single crystals irradiated with electrons and protons. Phys Solid State. 2002;44:274–7.
41. Mikhailov MM, Neshchimenko VV, Yuryev SA, Sokolovskiy AN. Investigation of Optical Properties and Radiation Stability of TiO2 Powders before and after Modification by Nanopowders of Various Oxides. In: Yang D, editor. Titanium Dioxide - Material for a Sustainable Environment, InTech; 2018. p. 485-504.
42. Mikhailov M, Neschimenko V, Sokolovskiy A. Features of degradation and recovery of the optical properties of coatings based on ZnO powder modified with nanoparticles after irradiation. Radiat Eff Defects Solids. 2018;173:198–209.
43. Mikhailov MM, Verevkin AS. Optical properties and radiation stability of thermal control coatings based on doped zirconium dioxide powders. J Mater Res. 2004;19:535–41.